Military Technical College
Cairo, Egypt

A. M. M. E.

12th International Conference
on Applied Mechanics and
Mechanical Engineering (AMME)

MECHANICAL CRITERIA FOR ROBOTS TO OPTIMALLY JUMP AND RUN

MOHAMED, M.A.S.

ABSTRACT

Various types of functions that robotic legs can carry out are reviewed, namely; walking, jumping, leaping, hopping, and running. General and specific features for each type of function are discussed towards pinpointing how to design proper paths. A simulation model for the leg linkage by an equivalent spring is proposed. The model's steady function is achieved by a chain of repeated cycles consisting of compatible segmented paths. Thus, an air segment is a symmetric part of a parabola, whereas a ground segment is a symmetric portion of a whole standard sinusoidal curve. Two numerical case studies reveal that no matter how the legs steadily function, the motion performed by contributing parts has to be based on three considerations. First, the path of the hip joint w.r.t. horizontal ground level should be well stated. Second, the base motion of the supporting leg axle is close to pure rotation about toe/ground adhesion point. Third, the relative contraction of the leg radius expresses the counterpart joints shaping angles and control moments relative to the leg axis. In addition, an appropriate motion designed for the other leg determines the specific type of the intended output function. The output function properly proceeds as long as the other leg is given the accurate time to recover its upcoming landing profile.

KEYWORDS

Displacement and speed compatibility, leg linkages, equivalent spring, recovery stage of the landing profile.

1. BACKGROUND

Although articulated legs of all creatures have a common simple structure with slight differences, they are still able to provide the carried body with numerous types of functions. These types may have steady features such as jumping, hopping, crawling, walking and running, or transient such as turning, kneeing, and pushing objects [1,2]. The problem of analyzing these different types of functions is the theme of numerous current researches in a variety of fields [3-5]. It represents a rich topic in biomechanics of leg substitute, rehabilitation devices of handicapped individuals, and mobile robots applications [6,7]. For a quite long time, even mobile robots on horizontal level have captured a limited interest of researchers [8,11]. Nowadays however, a pronouncing need for machines traveling on irregular terrains, especially in space planets exploration, brainstorms researchers to in-depth tackle and compete over the subject matter of robot running and jumping [12,13].
Once a research project elaborates on the robot running topic, related practical aspects call for a joint contribution of numerous fields such as automatic control, vision devices, and computational mechanics. In addition, the project team should check itsapproach based on similarity to live creatures and review other different functions. This challenge makes impossible to come up with a simple convincing model to describe most of leg functions [14,15].
In the present study, we put forth a simple and comprehensive model to outline common mechanical aspects met in jumping and running functions. Without a loss of generality, the model includes a set of assumption based on real evidences observed with the traveling bodies and their carrying leg linkages. Governing equations of motion derived from the model are then analyzed in order to satisfy not only theoretical constraints of the body's path compatibilities but also operational requirements of joints' powering devices.

2. MOBILE ROBOTS

One common issue in a robot system is to design the path of the end effector. In general, a path satisfies the time displacement requirements for the end effector to start from one initial spot and to stop at a destination assigned. Owing to space constraints, the path often consists of a number of time segments. In order to reduce robot end vibration, smooth shifts via connected segments imply that segments' boundaries be compatible in terms of displacements and speeds. Further computations towards a refined path call for selection of well known analytic functions for such time segments. For a robot's leg linkages, our concern is to provide a traveling mass with a type of intended motion similar to that performed by live creatures. Main requirements of the intended motion for both mass and linkage should be properly stated first;

a) motion has a distinct unit cycle
b) repetition of the cycle yields a continuous function
c) only two similar sets of linkages are to carry out the intended motion of the traveling mass
d) the two linkage sets function independently
e) the motion cycle of each set is overlapped with that of the other
f) the set has some constraints on the angles direction and limits

g) the traveling mass is either in a projectile path or in a spring-supported ground path. The mass should alternate between the two paths.
h) the motion cycle of a linkage consists of two segments; being the hung stage and the support stage. The linkage is hung during two successive projectiles besides the support stage of the other linkage in between. The linkage carries the traveling mass during its one support stage. Thus the hung stage lasts longer than the ground stage.
i) In the hung stage the mass carries the linkage. In the support stage the linkage carries the mass.
j) In the air segment of the mass, both linkages are hung. In the ground segment of the mass, one leg is hung whereas the other carries the mass.

In our present study we havethree tasks; namely

a) to describe the plane motion of the traveling mass, along the vertical axis in jumping, and along a horizontal ground level in running
b) to describe the base motion of leg axis w.r.t. hip joint
c) to describe the relative angular motion of the supporting linkages

Linkage absolute motion consists of two combined parts, being base and relative. The base motion is pure rotation of the main axis about a given point. This point is either stationary at the toe/ground contact adhesion or traveling at the main hip joint. The relative motion is a set of link angular swivels of the three joints. It should be reminded that these joints are always provided with muscle moments to ensure a leg consistent form.

3. EQUIVALENT SPRING

3.1 Functional Similarity of Legs and Springs

While jumping and running, elevation of the human body above ground shows a well distinct cyclic behavior. This remark inspires that the leg linkage carries out a synchronized motion which makes the human body appear as if it bounces on an elastic medium. In other words, replacement of the leg linkage by an elastic spring may lead to the same observed type of motion of the traveling body in reality. In addition, jumping and running functions cause that the body undergoes kinetic/potential energy conversion, elastic impact and shocks, and momentum conservation. Since the linkage is not flexible and damage rarely occurs, the joint angles and moments should behave exactly like a protective spring. The real application of this robot has still the leg linkages feature. Instead of the spring, we gradually apply its equivalent forces by the joint moment. The resulting displacements ensure safe landing of the supported body.

3.2 Span Radius and Joints Shaping Angles

Let us define the axle line of a leg as the line extended between two extremities; namely, the body-hip joint the foot-toe joint. The toes function is mainly to provide the leg axle with a larger ground contact area. While man stands upright, the span radius is

$$r_0 = \left[(\ell_1 + \ell_2)^2 + \ell_3^2 \right]^{0.5} \quad (1)$$

where $_i$, i=1, 2, and 3 are link lengths. At this special position, the moments at joints, M_i, i=1, 2, and 3, can be controlled so as to ensure a balance between the body weight and the feet ground reaction; both acting along the span axis. Each selected set of joint moments provide joint angles that reshape the linkage as a rigid skeleton with reduced span radius $r(\theta_1,\theta_2,\theta_3)$. The compressive force F and its reaction along the defined span line are readily derived from the joint moments, or vice-versa. Joints angles are shaped mainly by the joints holding moments. Suppose that we are able to select these moments so that the end force F becomes linearly proportional with the span net contraction $d(\theta_1,\theta_2,\theta_3)$, i.e. $F(M_1,M_2,M_3)=k\ d(\theta_1,\theta_2,\theta_3)$, where k is a proportionality constant. Under such conditions, the leg linkage can function as a linear spring. Upon exerting a compressive force at the two extremities, the skeleton reshapes with different angles at joints and its span length contracts as a deflection function $d(\theta_1,\theta_2,\theta_3)$. Whether the leg hung in air or adhered to ground to support the traveling body, its span radius may vary from full extension to full contraction and back to full extension. Neither friction damping nor energy loss is considered in joints. Practically however, moments of joints are spontaneously powered and automatically fed so as to compensate friction losses and the friction appears as if it is absent. Fig.(1) shows two main geometrical relationships connecting the shaping angles as the span length changes from r_0 to r(t) given as;

$$r(t) = \ell_1 \cos\theta_1 + \ell_2 \cos(\theta_2 - \theta_1) + \ell_3 \sin(\theta_3 + \theta_2 - \theta_1) \quad (2)$$

$$\ell_1 \sin\theta_1 + \ell_3 \cos(\theta_3 + \theta_2 - \theta_1) = \ell_2 \sin(\theta_2 - \theta_1) \quad (3)$$

Adopting an intended similarity with human legs proportions, limiting constraint values are introduced as $-20^o<\theta_3<20^o$, $0^o<\theta_2<140^o$, and $-40^o<\theta_1<120^o$. Accordingly, the leg full extension and full contraction can be derived. Therefore, based on a preliminary graphical scheme for each type of legs motion application we start with the evaluation of changes in leg span radius as a time function, e.g. r(t). Next, an experimental plotting of the function $\theta_1(t)$ is traced. The numerical plot is then fitted to the closest analytical function for better manipulation of further computations. Equating the side length KT of the triangles KTH and KTQ in Fig.(1), the functions $\theta_3(t)$ and $\theta_2(t)$ are readily derived as;

$$\theta_3(t) = \sin^{-1}(w) \quad (4)$$

where

$$w = \frac{\{r(t) - \ell_1 \cos\theta_1(t)\}^2 + \{\ell_1 \sin\theta_1(t)\}^2 - \{\ell_2^2 + \ell_3^2\}}{2\ell_3\ell_2}$$

and

$$\theta_2(t) = \gamma(t) + \theta_1(t) \quad (5)$$

where

$$\gamma(t) = \delta(t) + \sin^{-1}\left[\{\ell_1 \sin\theta_1(t)\}\left\{\alpha^2(t) + \beta^2(t)\right\}^{-0.5} \right]$$

$$\alpha(t) = \ell_2 + \ell_3 \sin\theta_3(t) \quad (6)$$

$$\beta(t) = \ell_3 \cos\theta_3(t)$$

$$\delta(t) = \tan^{-1}[\beta(t)/\alpha(t)] \quad (7)$$

4. VERTICAL JUMPING

4.1 Distinctive Features

Close observation of human jumping shows that the human body continuously alternates along a vertical straight line path. Body jumping results from one single type of plane motion concurrently performed by the linkages of both legs. To prepare the body for jumping, joint strained muscles first reduce the leg radius and then legs fast extension provides the body with the proper launching speed. Accordingly, the body rises to reach an intended maximum height, storing a great potential energy. Gravity then brings the body down to ground level where a large amount of resulting kinetic energy should be absorbed. Legs work also as the only energy absorbing cushion responsible for protecting the body from shocks and vibration damages.

4.2 A Model Design

Fig.(2) shows a jumping model where a frictionless slider of mass m slips along a fixed vertical beam. At the slider's lower edge, a linear equivalent spring is attached whose rate is k. As the slider ends its free gravitational drop, a spring deflection starts as impact of the lower end with ground, then gradually increases during initial contact period, and ends as a sudden release (impulse) to push the attached mass up. While in air, the spring is not deflected i.e. it extends over its free length. As outlined above, deflections of the equivalent spring match the changes in the leg span radius from which the three joint shaping angles are derived based on eqns.(4,5).

4.3 The Model Assumptions

Since the legs are modeled as a spring, the modeled mass expresses the mass of real body with the legs mass ignored. This remark can be equally stated as the legs linkages or the equivalent spring is assumed weightless. In addition, impact is assumed to be elastic. Such an assumption, along with the above assumption of weightless legs, eliminates any loss in linear momentum or kinetic energy of the sliding mass at both instants of collision landing and impulse launching.

4.4 Governing Equations

Continuous jumping can be viewed as a chain of repeated cycles. A jumping cycle is an alternating motion along a fixed vertical line. The cycle consists of two segments,

being in air and on ground. Each segment is achieved along a path of two strokes. Thus, the vertical shift of hip joint y(t) during one jumping cycle is obtained from one of the four strokes, i.e.

$y(t) = \{y1, y2, y3, y4\}$ (8)

In the air segment of Fig.(2), we refer to the conditions of vertically thrown bodies for which we have;
$y1 > h_0$, air up stroke, $V_0 \geq V_y \geq 0$ against gravity
$y2 > h_0$, air down stroke, $0 \leq V_y \leq V_0$ gravitated
The speed is given by

$$V_y(t) = V_0 - gt, \quad (9)$$

and the traveled distance is given by

$$y(t) = h_0 + V_0 t - 0.5gt^2 \quad (10)$$

which is a part of a parabola. The gravity field ensures that
elevation time $= \bar{t}$ = falling time $= \bar{t} = V_0/g$,
duration of air segment $= 2\bar{t} = 2\ V_0/g$,
$y(0) = y(2V_0/g) = h_0$ and
$V_y(0) = - V_y(2V_0/g) = V_0$.
The maximum elevated shift is

$$y_{max} = y(\bar{t}) = h_0 + 0.5V_0^2/g. \quad (11)$$

On the other hand, in the ground segment of Fig.(2) the hip elevation drops. The force analysis of the mass/spring system yields the differential equation

$$m\ddot{y} + ky = -mg, \quad (12)$$

with initial conditions
$y(0) = h_o, \dot{y}(0) = -V_o$

The solution is given as

$$y(t) = h_o - gm/k - Y\sin\left(t\sqrt{k/m} - \eta\right) \quad (13)$$

This shows that the ground sinusoidal segment is slightly more than a half standard cycle whose amplitude Y and phase shift η are given by;

$$Y = \left[(gm/k)^2 + V_o^2 m/k\right]^{0.5} \quad (14)$$

$$\eta = \tan^{-1}\left[g/V_o\sqrt{\frac{k}{m}}\right] \quad (15)$$

where m is the mass of the supported body (body mass without legs), duration of the total ground contact time= $t_c = [\pi + 2\ \eta]/[k/m]^{0.5}$, and maximum spring deflection occurs at 0.5 t_c, i.e.

$$y_{max} = y(0.5\ t_c) = -Y - gm/k \qquad (16)$$

which is a symmetric part of a whole standard sinusoidal cycle. This ensures that $y(t_c)= h_0$ and $V_y\ (t_c)=+ V_0$. In short, we simply have:
y3 < h_0, ground down stroke, $V_0 \geq V_y \geq 0$ storing the elastic energy, and
y4 < h_0, ground upstroke , $0 \leq V_y \leq V_0$ release of elastic energy.
For the ground segment: entrance speed is $V_o\downarrow$ and exit speed is V_o . Thus, the ground sinusoidal segment is compatible at both its side boundaries with the two boundaries of the air parabolic segment in terms of speeds and displacements. Therefore the jumping cycles can be smoothly connected as a chain for continuous jumping. In other words, the boundary conditions at the two sides of each segment are compatible with those boundaries of the preceding and the following segments. In addition, repetition of the jumping cycle implies that exit boundaries of the fourth stroke are compatible with the entrance boundaries of the first stroke.
It is noticed that whether the hip joint passes by the height h_0 upwards or downwards, the absolute value of speed is always V_0. Thus, the jumping cycle resembles a pendulum motion. However, the pendulum cycle follows a whole sinusoidal path, whereas the jumping cycle follows a piece-wise path consisting of an air parabolic segment properly connected to a ground sinusoidal segment. Finally, In order to evaluate the rate of equivalent spring we express the principle of conservation of energy at the landing instant and midpoint of the support stage; i.e.

$$0.5mV_0^2 + mgd_{max} = 0.5kd_{max}^2$$

$$mg(h_{max} + d_{max}) = 0.5kd_{max}^2 \qquad (17)$$

$$\frac{k}{m} = 2g\frac{h_{max} + d_{max}}{d_{max}^2}$$

Thus the ratio k/m should be properly selected based on the allowable linkage deflection d_{max} and the desired elevated height h_{max}. In addition, the ratio k/m expresses the angular speed of the sinusoidal segment.

4.5 A Numerical Example (Jumping)

Let us take the case of V_o = 4.9 m/sec, d_{max} = 0.5 meter, h_{max} = 1.22 meter, k/m=135.25 radians^2/sec^2, r_0= 1.1 meter, $_1$=0.6, $_2$=0.4, $_3$=0.2 meters. Fig.(3) shows the time variation of hip displacement and speed over one jumping cycle. It is clear that duration of the ground segment lasts longer than the air segment by about 12%. Obviously, other numerical values yields different durations ratio. However, the limit values of joint angles set the constraints of the duration ratio. To get the shaping angles during the ground segment, we first substitute r(t) =y(t) in eqns.(4,5). Next, a linkage graphical sketch is used to guess the time dependence of the function $\theta_1(t)$, from which a numerically fitted $\theta_1(t)$ was found to be close to

$$\theta_1(t) = 32 \cos \{\pi [y(t) - \ _1] \} + 5 \qquad (18)$$

The linkage unloaded configuration is chosen with all joint angles slightly swiveled from the upright standing state. For instance, the link $_1$ is provided with an initial inclination angle $\theta_1(0)$ =5° w.r.t. the vertical path of motion. This initial articulated form avoids shock adverse effect on joints, reduces compressive stresses induced in links, and helps further angular swivels to smoothly proceed.

The time variation of the set of shaping angles $\{\theta_i(t)$, i=1,2, and 3$\}$ are plotted in Fig.(4). As already observed in human jumping, the figure shows that maximum angular swivels occur as the body passes the lowest height. In addition, the knee angle $\theta_2(t)$ generally undergoes the largest angular swivels compared to $\theta_1(t)$ and $\theta_3(t)$.

5. PLANE RUNNING

5.1 Distinctive Features

The running main objective is to achieve continuous horizontal traveling with a fast pace. Most distinctive features of human jumping mentioned above are also embedded in the running function. Nevertheless, running still has its own three supplementary features, being oblique velocities of the body, base rotational motion of one supporting leg axles, and continuous and independent variation of both legs radii. Analysis of running reveals that as the body obliquely lands, one of the two legs' toes adheres to ground in order for the leg axle to be prepared to provide a proper supporting ground reaction. Thus, the leg axle leans to make an acute angle with horizontal level. Next, leg joint muscles should be gradually strained and leg radius contracts first to soften joint impact and to absorb body kinetic energy. Then the joint angles rapidly restore the no-swivel values in order for leg radius to recover its longest span. Both contraction and extension of the leg radius are combined with the rotation of the axle about the toe/ground adhesion point towards a final obtuse angle. This action provides the body with a proper launchingspeed . The final velocity vector here should be oblique to ground to ensure both horizontal traveling and a convenient height elevation. As in the case of jumping, the whole body will gain a flight segment but for a shorter time and a lower height. Reduction in flight time and height is a direct result of two factors. First, energy is only a half since it is supplied by just one leg linkages. Second, a significant part of this half energy is reserved towards horizontal traveling.

5.2 A Model Design

The jumping model outlined above can be slightly modified to construct a running model as in Fig.(5). The body in air moves as a plane motion of a free body in the gravitational field. Upon oblique ground landing, the body is hooked to a slider, relatively slipping along an acutely slanted rigid beam. The beam starts a base motion of pure rotation about the toe/ground adhesion point. Relative position of the slider on the beam is controlled by a linear spring working along the beam axis.

5.3 The Model Assumptions

As the leg linkages move relative to the body, the body overall center of gravity continuously changes its location. This introduces a rotational component to the plane motion of the body. Seeking a simple model, let us assume that leg linkages are weightless. Thus, the body whole weight is concentrated at the hip joint of legs. Accordingly, no matter how the linkages are shaped in air, the body gravity center is unchanged. This assumption eliminates violation of the projectile trajectory in air. In addition, the assumption of weightless linkages eliminates their mass moment of inertia in moment equations. Practical observations of human running emphasize the absence of body plane rotation.
During the ground stroke, the beam supports the body weight by a frictionless normal reaction and concurrently rotates with a uniform angular speed about adhesion point, i.e. zero angular acceleration. This means that moments of joints about the adhesion point balance the normal reaction moment at the hip joint. As will be justified in section (5.5), both these moments can be ignored.
In addition, ignoring the links mass eliminates noticeable contributions of the leg axle variable positions, whether as a support or a hung leg, to the rotating moment of the carrier beam. Thus, the beam rotates about toe/adhesion point mainly due to a transferred angular momentum. Other sources of moments are insignificant; namely, body weight, weight of hung and supporting legs, and pushing force of the other leg, joints moments.

5.4 Governing Equations

Close observation of human running reveals that a distinct running cycle consists of two time segments, one in air segment and the other on ground. In the air segment, the body follows a projectile path with an ascending stroke and an descending stroke. In the ground segment, the body follows a combined motion close to a spring/mass system. Continuous running is achieved as a chain of such dual cycles, each being performed by one leg at a time. For instance, after the right-leg provides the traveling body with its cycle, the left-leg starts its own cycle and so on. The ground segment performed in one leg cycle consists of two strokes, being the energy absorption stroke and the energy feeding stroke. As a leg linkage finishes its ground stage, it has to recover itsoriginal landing profile being so shaped to prepare for its upcoming ground stage. Thus, the Landing Profile Recovery Stage (LPRS) for a given leg lasts for its own contribution air segment plus the whole duration of the other leg cycle. While running, whether any leg is hung in air or supports ground contact, its span radius undergoes continuous variation from full extension to full contraction and back to full extension. Both leg linkages' span radii always shrink in lengths, making the joint angles reshape accordingly.

5.5 The Support V Stage (Switch)

During a leg/ground adhesion, rotating moments of the supporting leg arise from the parts weights, joint moments, and angular momentum of the body. A preliminary observation of the walking function reveals that the leg rotation is due to either a pushing hip-force supplied from the other leg in the acute stroke, or weight of body plus weight of the hung leg in the obtuse stroke. A leg in this stage positively contributes to the motion of the traveling body. By the appropriate moments, its joints angles are properly shaped to feed the body with the required launching speed. During running however, rotation of the supporting leg is solely due to angular momentum transferred from linear momentum of the falling body. Fig.(5) shows one leg in its ground support stage. The leg toe adheres to ground at point P with a slope angle ϕ_0. The leg axle rotates clockwise to make angle $\phi(t)$ with the negative x-axis. Assume the variation of axle radii be r(t) as a time function. Let (x, y) be coordinate components of the hip joint at a time lapse (t) after a landing starts. Analysis of forces on the body leads to two equations of plane motion

$$\begin{aligned} -k\,d(t)\sin[\phi(t)] + m\,g - R\cos[\phi(t)] &= m\,\ddot{y}(t) \\ -k\,d(t)\cos[\phi(t)] + R\sin[\phi(t)] &= m\,\ddot{x}(t) \end{aligned} \qquad (19)$$

where

$$\begin{aligned} d(t) &= r_0 - r(t) \\ y(t) &= h_0 - r(t)\sin[\phi(t)] \\ x(t) &= \bar{x} - r(t)\cos[\phi(t)] \end{aligned} \qquad (20)$$

It should be reminded that both ground adhesion and joints moments have small values compared to body weight. In steady walking the rotating moment of the supporting leg about the ground adhesion point depends on the value of slope angle φ. When $\varphi < \frac{1}{2}\pi$, the moment is principally due to rear leg pushing force at the upper hip joint. When $\varphi > \frac{1}{2}\pi$ the rotation moment is primarily supplied by the weight of traveling body. Thus, the moment of joints of the supporting leg is null as a source of body reaction R.

In early starting strokes of running when $\varphi < \frac{1}{2}\pi$, the rotation of leg axle of the supporting leg is due to joint moment developed about toe/ground adhesion point and transferred as reaction R to the traveling body. Thus, this moment is essential, and thereby under such conditions the reaction is a main component in the equations. But when $\varphi > \frac{1}{2}\pi$, the rotation moment is mainly supplied by the weight of traveling body. On the other hand, as steady running proceeds however, momentum of falling projectile (traveling body) is sufficient to cause the axle to rotate about the adhesion point. Accordingly the joint rotational moment has no need to be exerted, and thereby the reaction R may be safely neglected, especially for large angles ϕ, e.g. $75^o > \phi > 85^o$. Based on the foregoing analysis, adhesion moment of the supporting leg has insignificant effect on motion parameters. Canceling the slight effect of R leads to the two differential equations

$$\begin{aligned} m\ddot{y} + ky &= mg + kh_o - kr_o \sin(\dot{\phi}t + \phi_o) \\ m\ddot{x} + kx &= k\bar{x} - kr_o \cos(\dot{\phi}t + \phi_o) \end{aligned} \tag{21}$$

Referring to eqn.(21), when $\varphi < \frac{1}{2}\pi$ the spring and weight reduce the speeds, and when $\varphi > \frac{1}{2}\pi$, the spring and weight enhance the speeds. Now to include the boundary conditions we assume that landing from a foregoing projectile segment occurs at t=0. Thus, with the origin set at the hip joint we get

$$x(0)=0,\ y(0)=0,$$
$$\dot{x}(0) = v_x = v\cos\vartheta_0, \dot{y}(0) = v_y = v\sin\vartheta_0 \tag{22}$$

where V_x and V_y are components of the velocities at right end of projectile segments. Geometry shows that $\bar{x} = r_0\cos\phi_0$ and $h_0 = r_0\sin\phi_0$. Let $2\bar{t}$ be duration of ground contact. Based on the compatibility at the end of this ground segment and the start of the upcoming projectile segment at the instant $2\bar{t},$ we have

$$\begin{aligned} y(2\bar{t}) &= y(0) = 0, \\ \dot{x}(2\bar{t}) &= \dot{x}(0) = v_x, \\ \dot{y}(2\bar{t}) &= -\dot{y}(0) = -v_y, \end{aligned} \tag{23}$$

Velocity diagram at the end of ground segment implies that the slope angle of the leg axis is $\pi - \phi_0$. In addition, the path is symmetric about the midpoint $(\bar{t}, \bar{x})$. Assuming a constant angular speed rotation, thus

$$\dot{\phi} = (\pi - 2\phi_0)/2\bar{t} \tag{24}$$

Conservation of energy implies that

$$\frac{1}{2}m\,v^2(0) + m\,g\,y_{max} = \frac{1}{2}k\,y_{max}^2 + \frac{1}{2}m\,v_x^2(\bar{t}) + \int_{\phi_o}^{\pi/2} R\,r\,d\phi \tag{25}$$

The integral term is the work done to rotate the beam. However, since the kinetic energy has the same value at the entrance and exit instants, the reaction has no energy contribution and will be dropped. We use this equation to express the rate of equivalent spring k for a given body weight mg. The solution of the two differential equations is

$$\begin{aligned} y(t) &= A\sin(\omega t) + B\cos(\omega t) + C - D\sin(\dot{\phi}t + \phi_0) \\ x(t) &= E\cos(\omega t) + F\sin(\omega t) + \bar{x} - D\cos(\dot{\phi}t + \phi_0) \end{aligned} \tag{26}$$

where

$$\omega^2 = k/m$$
$$A = \left[v_y + D\dot{\phi}\cos\phi_0\right]\omega^{-1}$$

$$
\begin{aligned}
B &= -C + D\sin\phi_0 \\
C &= g\omega^{-2} + h_0 \\
D &= r_0\left[1 - \{\dot{\phi}\omega^{-1}\}^2\right]^{-1} \\
E &= -\bar{x} + D\cos\phi_o \\
F &= \left[v_x - D\dot{\phi}\sin\phi_o\right]
\end{aligned}
\qquad (27)
$$

At maximum deflection, the spring axis is vertical and $r(\bar{t})=r_o- y_{max}$. The vertical component of speed $V_y(\bar{t})=0$ and the resultant speed is horizontal given as pure rotation with zero rate of length contraction, i.e.

$$v_x(\bar{t}) = \dot{\phi}[r_0 - y_{max}]. \qquad (28)$$

From which the equivalent spring rate is corrected.
Knowing x(t) and y(t), the span radius is

$$r(t) = \left[\{h_0 - y(t)\}^2 + \{\bar{x} - x(t)\}^2\right]^{0.5} \qquad (29)$$

valid in the range of ground contact time $0 \le t \le 2\bar{t}$. Notice that the set of six boundary conditions yields an involved relationship to find the unique unknown, being the contact time $2\bar{t}$. Although an analytical solution is hard to manipulate, a graphical plotting along with an iterative scheme proves useful to arrive at a good numerical solution of contact time. The algorithm is as follows;

(a) select a value to the maximum difference in kinetic energy
(b) select a reasonable maximum deflection
(c) compute k/m, ω
(d) select ϕ_o
(e) assume a contact time close to the 0.5 of spring period $2\pi/\omega$
(f) compute $\dot{\phi}$
(g) plot the function y(t), and find its first two zeros referring to $t=0$ and $t_c=2\bar{t}$
(h) find resultant landing speed
(i) find slope angle (direction of landing, common tangent to both segments at connection instant.
(j) Iterate around the contact time until the six constraints are satisfied.
(k) Find the leg radius variation and the joints angles

The last algorithm proves successful to find the contact time as 0.568 seconds. However the method is still tedious and highly sensitive due to involved trigonometric functions.

5.6 The Hung Stage (Switch)

In section 5.4 we discussed the landing profile recovery stage. The base motion of the leg axle is pure rotation anticlockwise. The joints moments have to support the

leg links weight only. While the spring axis rotates, the length of equivalent spring is contracted to help the spring length pass through the contracted length of the other contacting spring. Thus, the hung leg should be shorter than the supporting leg. As long as the body is stable during single-leg ground contact, any symmetric variation of hung leg radius can be chosen as an arbitrary time function subject to a set of constraints. For instance, it is suitable to select a cosine variation over one period given as

$$\begin{aligned} r_{max} &= r_0 \\ r_{min} &= r_0 - y_{max} - \text{clearance} \\ r_{mean} &= 0.5(r_{max} + r_{min}) \\ &= 0.5(r_{max} - r_{min}) \end{aligned} \quad (30)$$

Thetime variation of the leg radius is

$$r(t) = r_{mean} + \quad \cos[2\pi\, t/(\, t_c + 2\, t_a)] \quad (31)$$

5.7 A Numerical Example (Running)

Let us take the case of V_o =1.06 m/sec, h_{max} = 0. 007 meter, d_{max} =0.216 meter, k/m =78.78 radian^2/sec^2, r_0= 1.1 meter, $_1$=0.6, $_2$=0.4, $_3$=0.2 meters, θ_0= 20^o, ϕ_0= 76.4^o, $\dot{\phi}$=0.8 radian/sec. Fig.(6) illustrates the body displacements, whereas Fig.(7) shows the plane trajectory of the body hip. Fig.(8) illustrates the speeds of the traveling body, whereas Fig.(9) shows the pattern of the joints shaping angles of one leg over its own single running cycle. It can be noticed that the hung segment levels are higher than the support segment levels. To visualize the dual cycle of the continuous running, an identical cycle superimposed from the other leg should be added to the plot. The ground stroke of one leg overlaps the mid position of the Landing Profile Recovery Stage of the other leg.

6. ANALYSIS AND DISCUSSION

Real observations show that common features in jumping and running are the ground and air strokes. In jumping all energy is directed to elevate the body. In running, part of energy is directed to achieve the horizontal component of displacement. Duration ratio of air/ground strokes is shorter in running than in jumping due to reduction in the vertical component of speed. The model can be applied to analyze other types of motion such as human walking and animal running. Animals use the same running cycle in two forms. When they use only one rear pair of legs, the linkages of both legs move paralleled to each other, running proceeds as a chain of a repeated cycle by the same pair of legs. When they use one front pair and one rear pairs of legs, running proceeds as a chain of dual cycles, one is performed by the front pair and the other by the rear pair.

We showed that the trajectory of the running body, equivalently of the hip joints, is a repeated set of cycles. This cycle consists of two main segments, namely; the ground segment and the air segment. The two segments should be compatible at their

boundaries in terms of displacements and speed. Since the whole body, including the leg links, has no contact with ground, the air segment should necessarily be a projectile. The ground segment may take numerous profiles depending on the sophistication used to model the motion dynamics. The segment is chosen symmetric with respect to the mid point. However, such a choice is not compulsory and accordingly, other profiles can satisfactorily meet the compatibility conditions. Just to name a few, we may use the part of an asymmetrical complex sinusoidal function, obtuse angle of landing, and two spring deflections separated by a pure rotation.

In the ground segment, one leg remains hung to the body, while the other leg is responsible to provide adhesion, stability in three planes, reactions versus gravity, energy absorbing and leg rotating moment, and impact and launching momentum. Exact moments come from gravity forces and the three link joints. However, due to short duration of ground segment, the contribution of link moments and weights is insignificant compared to that of angular momentum. The joints moments are mainly responsible for shaping the leg angles as a function of the required forces of the rate of the equivalent linear spring.

Running curve can be observed from another view point. Each leg has a distinct cycle. The cycle starts when the leg touches ground in the landing instant. The leg adhesion to ground and subsequent rotation provide energy and momentum requirements to the moving body to fly. Thus, in the subsequent air segment, this energy is consumed to perform the projectile segment. Although the second leg will soon land to perform its ground segment, the first leg remains hung to the main joint away from ground. In addition, the same first leg continues in the air until the end of the air segment of the second leg when it returns back to touch ground. As a result, the duration of a whole leg configuration is $2(t_c + t_a)$. Over the contact time t_c, the leg rotates anti-clockwise about ground adhesion point to shift the body horizontally from landing position to launching position (V switch), while its length switches from full extension to full compression and back to full extension. Over the period of $(t_a + t_c + t_a)$ the leg rotates clockwise about main joint hung to the body (switch), while its length switches from full extension r_o, shrinking to a shortened length of $(r_o - y_{max} -$ clearance), and back to full extension r_o, see Table (1).

7. CONCLUSION

The study tackles a very rich topic which needs a huge set of papers. An exact model has to perfectly match the well observed behavior of man legs. Since a simplified model full of assumptions still shows many computational challenges due to involved trigonometry, an exact model is expected to include extraordinary intricacies.

Jumping, walking, and running of a human body have the common feature of repeated unit curve. The unit curve describes the body motion while being in air or on ground. In air, the human body flies as any projectile whose trajectory is characterized by a number of well known parameters. The trajectory expresses the energy conversion from kinetic to potential and back to kinetic. In the initial position, speed and slope angle (launch angle) are given, other parameters are readily derived, such as maximum vertical altitude, landing coordinates, landing speed and

slope. Initial speed needs a type of energy to be supplied to the body. During ground segment, the leg linkage in ground contact has to receive the body momentum and energy. Impact implies that the coming linear momentum is transferred to angular and the supporting leg shrinks in net radius. Leg further rotation is controlled by gravity force and partly by joints moments. Shrink in radius is controlled by joint shaping angles and joint moments.

In this study, we put forth a simplified model with a set of acceptable assumptions. However, aiming at finding the exact contact time, the numerical solution of the model faces a sensitive iteration process of computations on commercial PC. Therefore, the model is recommended to study the running function on the academic and applied levels. For an extended detailed research, the present investigation still work as a nucleus of a highly sophisticated model. A realistic model will partially or completely exclude the set of proposed assumptions. In such a case, the huge expected set of linked exact relationships will lead to an involved computational scheme on a main frame.

REFERENCES

[1] Hun-ok Lim and Atsuo Takanishi, "Compensatory motion control for a biped walking robot, improved genetic algorithm for the permutation, flowshop scheduling problem," Robotica, Volume 23, Issue 01, pp 1-11, (2005).

[2] Elena Garcia and Pablo Gonzalez de Santos, "An improved energy stability margin for walking machines subject to dynamic effects," Robotica, Volume 23, Issue 01, pp 13-20, (2005).

[3] Katja D. Mombaur, Richard W. Longman, Hans Georg Bock, and Johannes P. Schlöder," Open-loop stable running," Robotica, Volume 23, Issue 01, pp 21-33, (2005).

[4] Zoppi, M., Zlatanov, D., and Gosselin, C.M., "Analytical kinematics models and special geometries of a class of 4-DOF parallel mechanisms," Robotics, IEEE Transactions on [see also Robotics and Automation, IEEE Transactions on], Volume 21, Issue 6, pp 1046- 1055, (Dec. 2005).

[5] Floreano, D., Zufferey, J.C. and Nicoud, J.D. "From Wheels to Wings with Evolutionary Spiking Neurons," Artificial Life, vol. 11, No1-2, pp. 121-138, (2005).

[6] Giuseppe Carbone, Yu Ogura, Hun-ok Lim, Atsuo Takanishi, and Marco Ceccarelli, "Dynamic simulation and experiments for the design of a new 7-dofs biped walking leg module," Robotica, Volume 22, Issue 01, pp 41-50, (2004).

[7] Chee-Meng Chew, and Gill A. Pratt, "Frontal plane algorithms for dynamic bipedal walking," Robotica, Volume 22, Issue 01, pp 29-39, (2004).

[8] Anjan Kumar Dash, I-Ming Chen, Song Huat Yeo, and Guilin Yang, "Instantaneous kinematics and singularity analysis of three-legged parallel manipulators," Robotica, Volume 22, Issue 02, pp 189-203, (2004).

[9] Chien-Chou Lin Chi-Chun Pan Jen-Hui Chuang, "A novel potential-based path planning of 3-D articulated robots with moving bases," Robotica, Volume 22, Issue 04, pp 359-367, (2004).

[10] Wisse M., Schwab A. L., and van der Helm F. C. T., "Passive dynamic walking model with upper body," Robotica, Volume 22, Issue 06, pp 681-688, (2004). [12] Yu Zhou, "On the planar stability of rigid-link binary walking robots," Robotica, Volume 21, Issue 06, pp 667-675, (2003).

[11] Wu Q. and Sabet N., "An experimental study of passive dynamic walking," Robotica, Volume 22, Issue 03, pp 251-262, (2004).
[12] Zhu, C., Tomizawa, Y., Luo, X., and Kawamura A., "Biped Walking with Variable ZMP, Frictional Constraint, and Inverted Pendulum Model," Proceedings of the 2004 IEEE International Conference on Robotics and Biomimetics (ROBIO2004).
[13] Vermeulen J., Lefeber D, and Verrelst B. "Control of foot placement, forward velocity and body orientation of a one-legged hopping robot," Robotica, Volume 21, Issue 01, pp 45-57, (2003).
[14] Chevallereau C.and Aoustin Y., "Optimal reference trajectories for walking and running of a biped robot," Robotica, Volume 19, Issue 05, pp 557-569, (2001).
[15] Zhu, C., Aiyama, Y., and Arai, T., "Releasing Manipulation with Learning Control," IEEE Robotics & Automation, pp. 2793-2798, (1999).

Table (1) Comparison of base rotational motions of a leg

Stage	V supporting leg	Λ hung leg
Spring upper end	deflected	Not deflected
Spring lower end	Not deflected	deflected
Max deflection	y_{max}	y_{max} + Clearance
Center of rotation	adhered to ground	Traveling with hip
Rotation angle Range	$\pi - 2\,\phi_0$	$\pi - 2\,\phi_0$
duration	t_c	$t_a + 2\,t_c$
Angular speed	Constant ϕ	Constant ψ
Spring axis rotation	clockwise	anticlockwise
Initial slope angle	$-\phi_0$	ϕ_0
Final slope angle	ϕ_0	$-\phi_0$

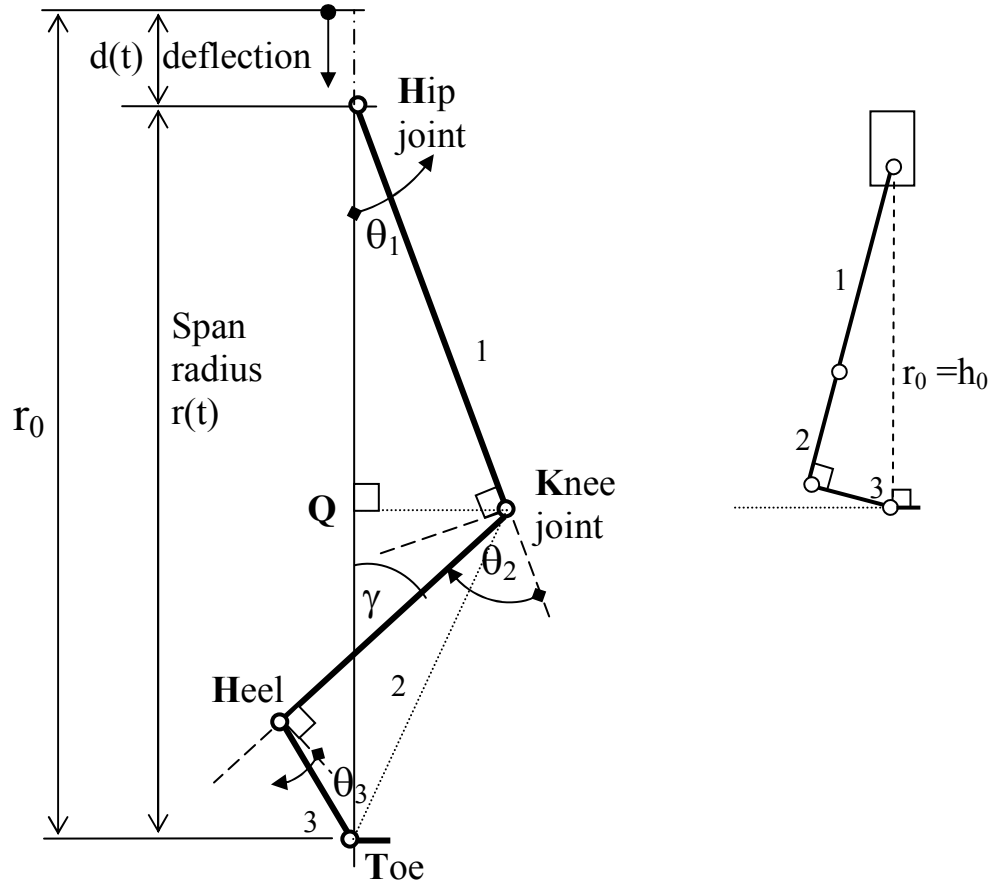

Fig.1 Joints shaping angles as hip approaches ground

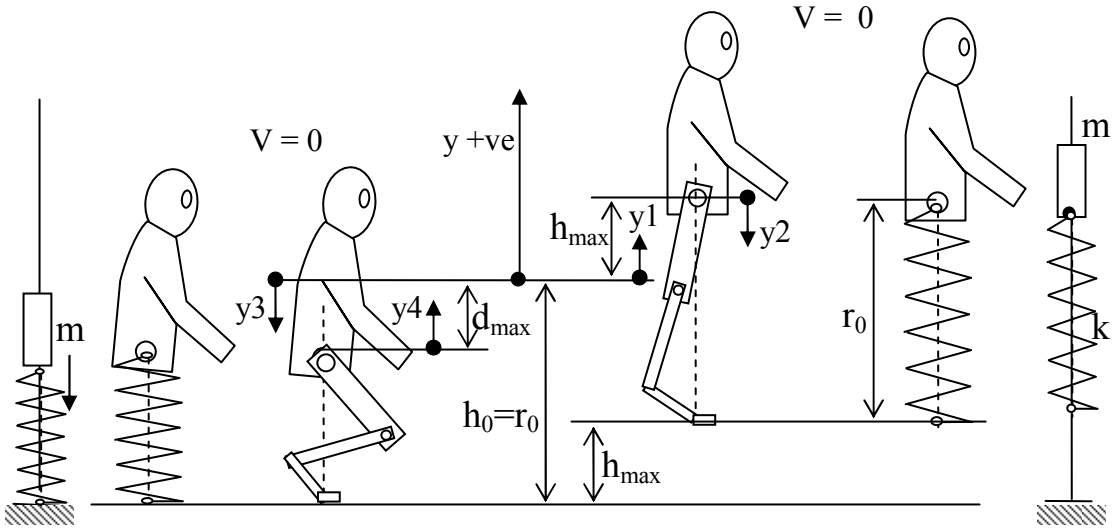

Fig.2 Hip elevation while jumping and equivalent spring

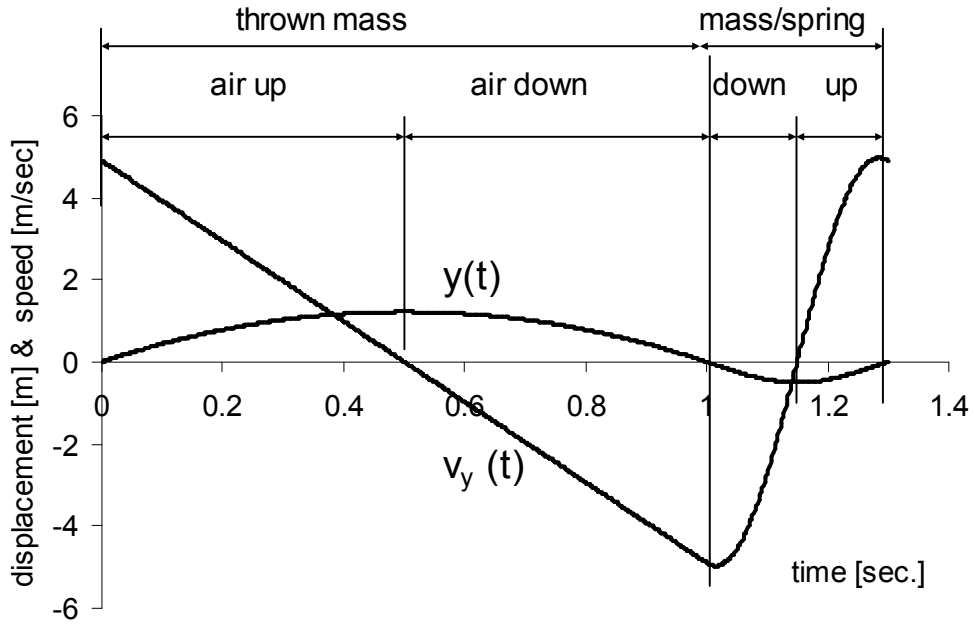

Fig.(3) displacement and speed for the four strokes of one jumping cycle

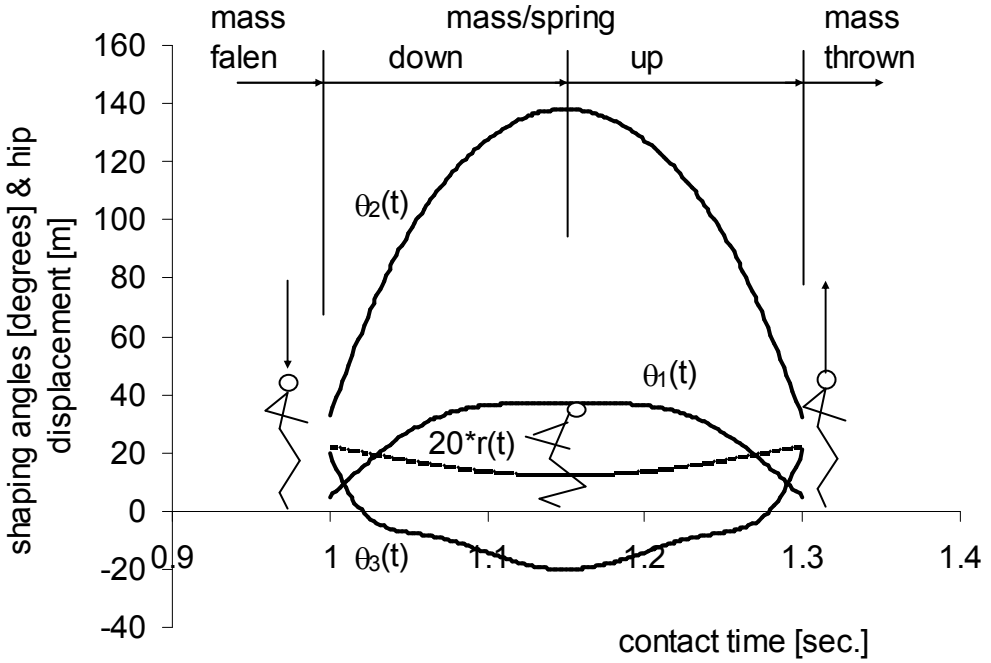

Fig.(4) joint shaping angles for the two ground strokes of a jumping cycle

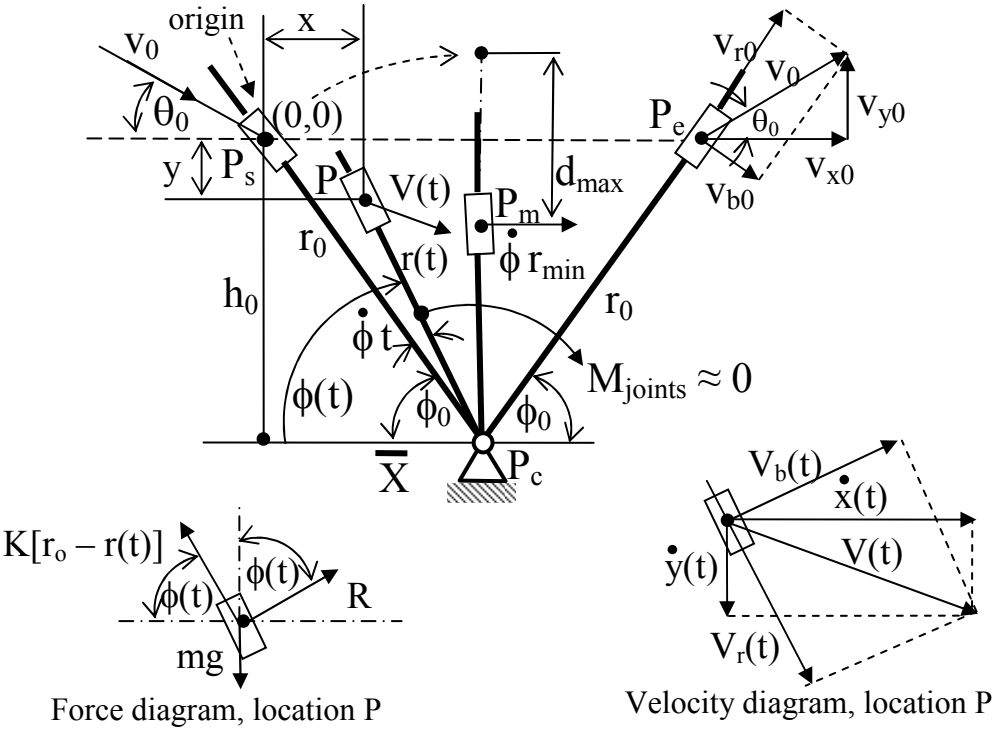

Fig.(5) Rotation of the supporting leg (spring axle) during ground time segment

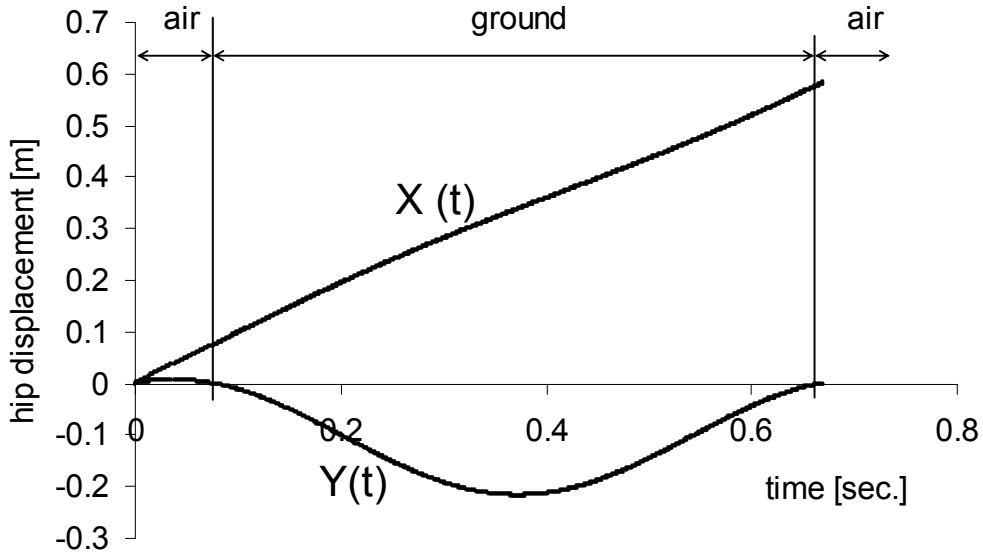

Fig.(6) Plane displacements of the body hip while running

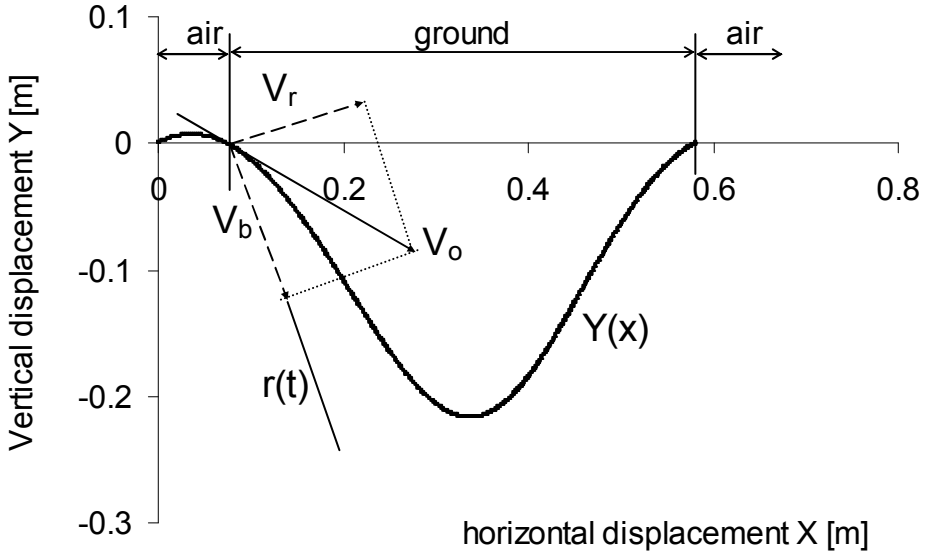

Fig.(7) Path trajectory of the body's hip while plane running

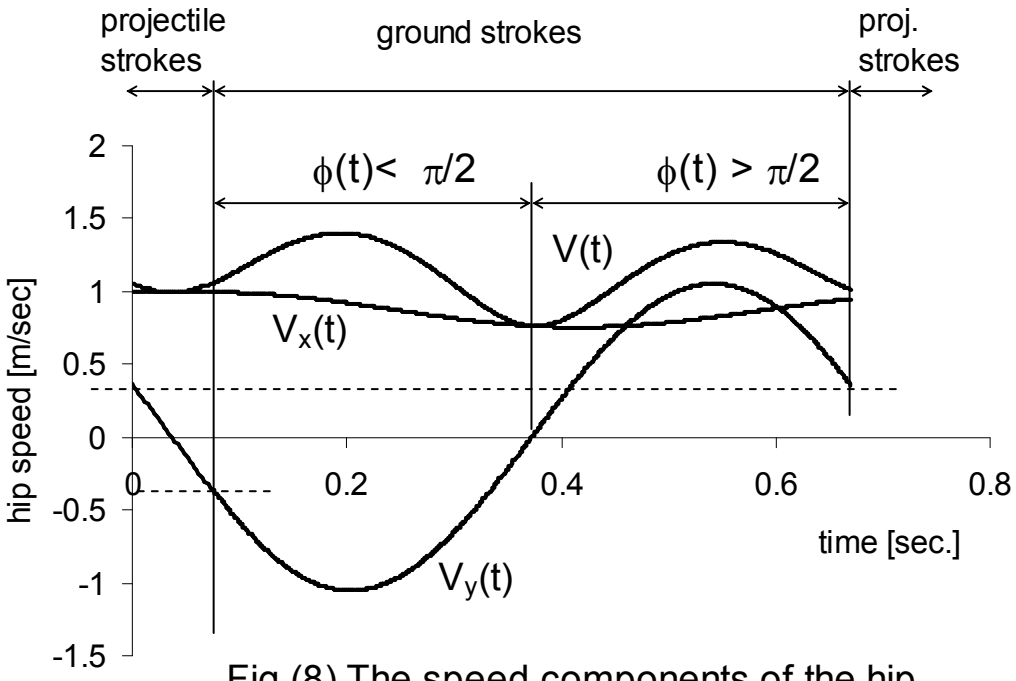

Fig.(8) The speed components of the hip joint during the two strokes of one running

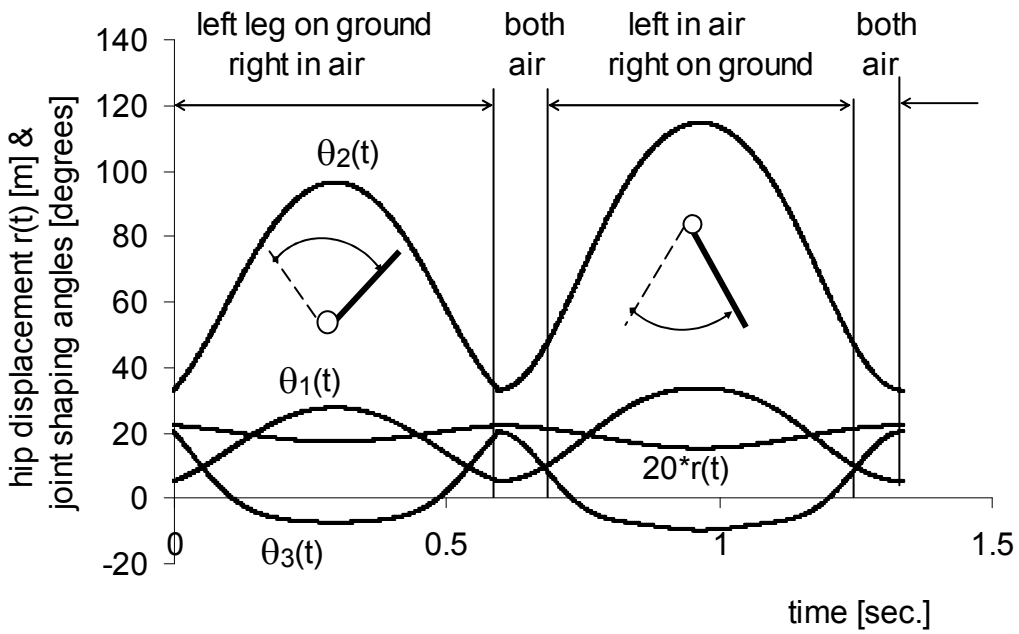

Fig.(9) Variation of joints angles during one running cycle